

A Geoinformatics Approach to Assess Land Use Dynamic and Landscape Fragmentation Due to Opencast Coal Mining in Raniganj Coalfield, India

Amit Sarkar

Senior Research Fellow, Department of Geography, University of Calcutta, Kolkata-700019, India

Email: iamitsarkar91@gmail.com

Abstract- Land use dynamics and landscape patterns have always been prime themes of global change research (R.H.U. & Suocheng, D. 2013). Anthropogenic changes in the form of opencast mining make the ecosystem more sensitive and fragmented. Miscellaneous mining aids like dumper, dozer and dragline caused enormous amount of land degradation. Indeed the degraded land covers are fragmented in due course of time. Raniganj coalfield area has a complex land use land cover fragmentation scenario due to opencast mining and associated development activities since 1960 (Das, G. & Das, R. 2016). Arc GIS and fragstats software is used in order to measure the class level and landscape level fragmentation of different landscapes in Raniganj coalfield and adjoining area since last 40 years. Results denote that most of the landscape classes have become fragmented and isolated. The areas of forest, agricultural land, excavated land and urban tend to be complex in their shape and spatial clustering. The shapes of other land class patches have become less complex, but overall landscape fragmentation has increased during last 25 years. Contrary landscape diversity and heterogeneity have also been increased within only 20 years especially in Sonapur Bazari, Satgram, Sripur and Khottadih area. Therefore it is urgently essential to understand and compute the land use fragmentation process in Raniganj mining area.

Keywords: opencast mining, class and landscape level fragmentation, fragstats and Arc GIS

1. INTRODUCTION

The researchers strive to interpret land use land cover fragmentation in the focal areas of Raniganj coalfield and its surroundings using remotely sensed data. Opencast coal mining affects the local landscape, adversely causes widespread environmental decay especially land alteration and fragmentation (Maitima, J.M., Mugatha, S.M., Reid, R.S., Gachimbi, L.N., et al. 2009). Therefore preparation and identification of land use land cover fragmentation in temporal manner for any particular area is very crucial nowadays in earth science in order to detect the temporal changes in land use land cover (State, J., Kumar, A. & Pandey, A.C. 2013). These fragmentation process put forwarded by mining and associated development activities are

measured by computing the 11 class level and 2 landscape level fragmentation indices.

2. RESEARCH AREA

Raniganj coalfield is located within four districts of West Bengal i.e. Burdwan (71%), Birbhum (9%), Bankura (8%) and Purulia (7%) shown in figure 2.1. This coalfield is elliptical in shape. East-west extension is about 75 km and north-south extension is about 35 km. It has an area of about 1530 sq km and falls within latitudes 23° 30' N to 23° 52' N and longitudes 86° 38' E to 87° 23' E. As on 2016 this coalfield has 17 running OCPs and 21 abandoned OCPs within 11 areas (ECL 2015). Mean elevation is 98.45m with broad undulation (Sarkar, A., 2016).

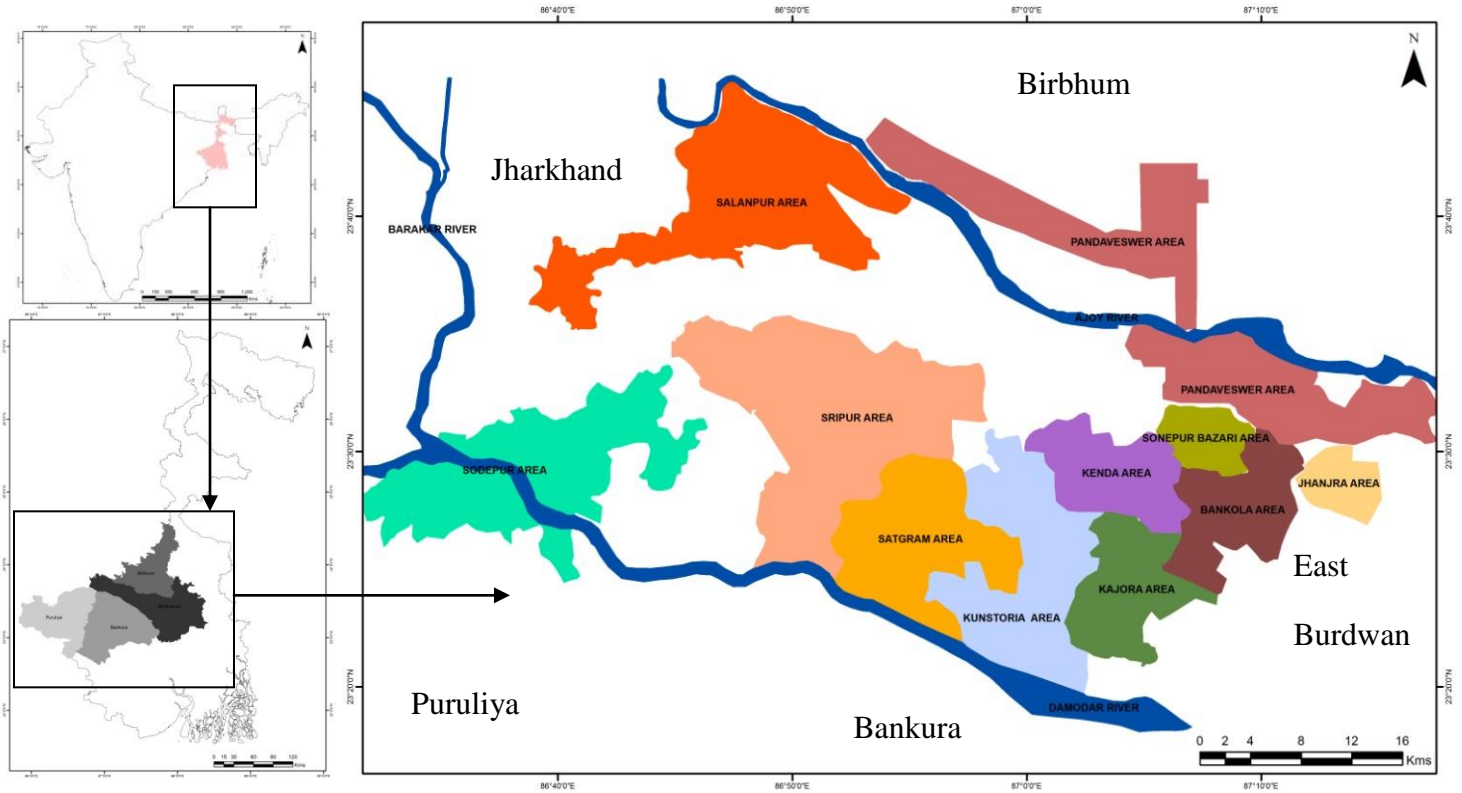


Figure 2.1: Location of Research Area (Source: ECL & CMPDI)

3. MATERIALS AND METHODS

3.1 Remote Sensing Data Sources

Five temporal cloud free satellite data is gleaned from USGS Earth Explorer portal in order to prepare land use land cover map from 1973 to 2015.

Information about satellite data is shown in table 3.1.1. Topographical maps with a scale of 1:50000 namely 73M/1, 73M/2, 73M/5, 73M/6, 73I/13 and 73I/14 from Survey of India is applied to build the base layer of these satellite data.

Table 3.1.1: Details of remote sensing satellite data, Raniganj coalfield

Year	Date of Acquisition	Path/Row	Spatial Resolution	Description	Projection
1973	18 th & 20 th March	149/44 & 150/43	60 m	Landsat MSS	World
1992	15 th March	139/44	30 m	Landsat 5 (TM)	Geological
2002	19 th March	139/44	30 m	Landsat 7 (TM)	Survey 84/
2010	25 th March	139/44	30 m	Landsat 7 (TM)	UTM, Zone
2015	15 th March	139/44	30 m	Landsat 8 (ETM+)	45

3.2 Data Processing

Data processing tasks are done from spatial and spectral enhancement menu of image interpreter tab

in ERDAS Imagine software. In order to extract the entire research area for the year 1973 image stretching is performed using mosaic tool from data

preparation tab (Sarkar, A., 2017). Image enhancement techniques like histogram equalization, contrast stretching and tail trimming are accomplished in order to improve the visual interpretability of remotely sensed image. RGB to IHS and the reverse IHS to RGB colour space transformation functions are also accomplished for the year 2002 and 2010 to extract more information.

3.2 Classification Scheme

Beyond of visual interpretation signatures are selected by using AOI tool followed by parametric statistical method from the signature editor menu bar with region growing properties in Erdas Imagine. Signatures are collected from multiple areas throughout the image for a single class and are merged which belong to the same class and renamed after a land use land cover class (Lillesand et al., 2004). In this manner ten distinctive land use land cover classes are captured. These are— forest, agricultural land, fallow land, river, river sand, water body, exposure, mining lagoon, urban and excavated. On average 125 forest signatures, 153 agriculture

signatures, 165 fallow signatures, 60 river signatures, 120 river sand signatures, 75 water body signatures, 87 exposure signatures, 50 lagoon signatures, 155 urban signatures and 80 excavated signatures are determined for one temporal image. Signature alarm and contingency matrix utility is also used to evaluate signatures that have been created from AOI in the image. After all these evaluations, supervised classification is performed with a distance file from classification tab/signature editor menu bar/classify/supervised to perform a supervised classification. Under parametric decision rule, maximum likelihood is selected. Then ok is clicked in the supervised classification dialog to classify the image (Sapena, M. & Ruiz, L.A. 2015). Post classification filtering is applied from the viewer menu bar/select raster/filtering/statistical filtering (median filter) to remove unwanted discrete pixels from the thematic image and to producing homogeneous region permanently. The classified maps for 1973, 1992, 2002, 2010 and 2015 are shown in figure 3.2.1, 3.2.2 and 3.2.3 respectively

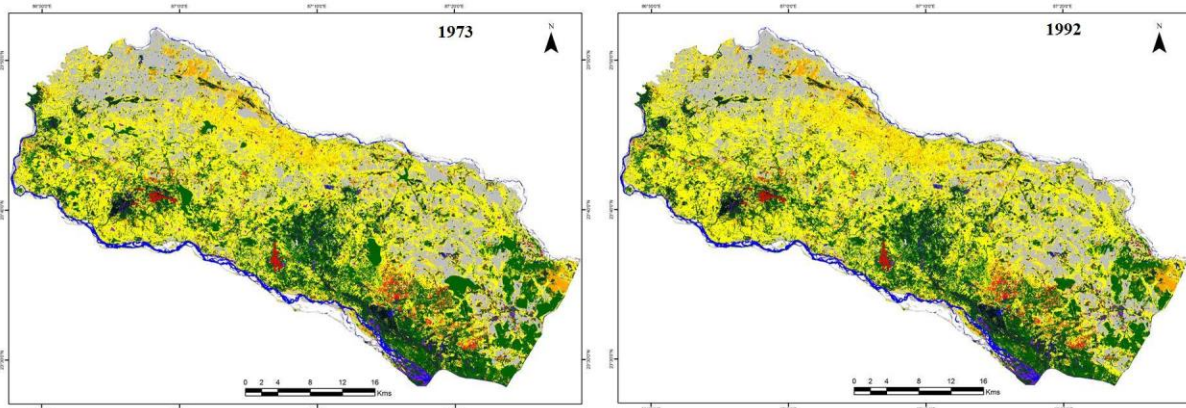


Figure 3.2.1: Landscapes map of 1973 and 1992 (clock wise), Raniganj coalfield

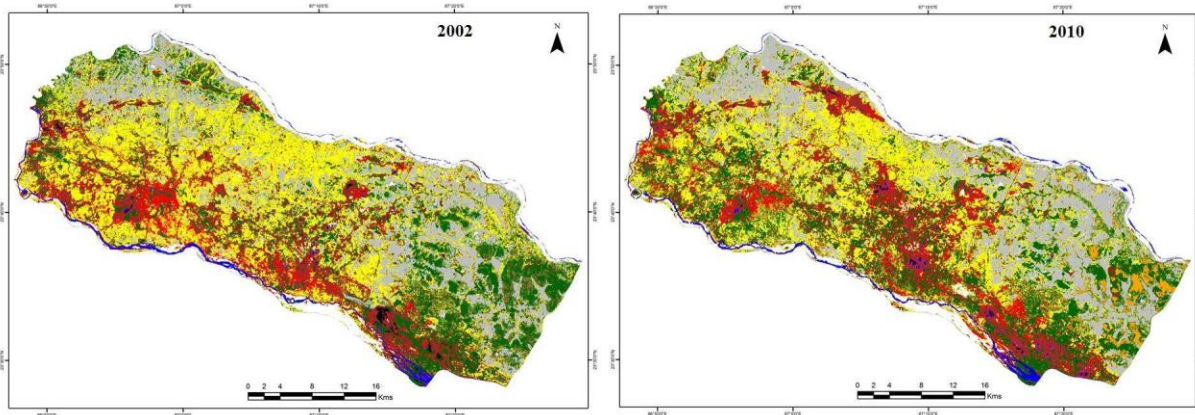


Figure 3.2.2: Landscapes map of 2002 and 2010 (clock wise), Raniganj coalfield

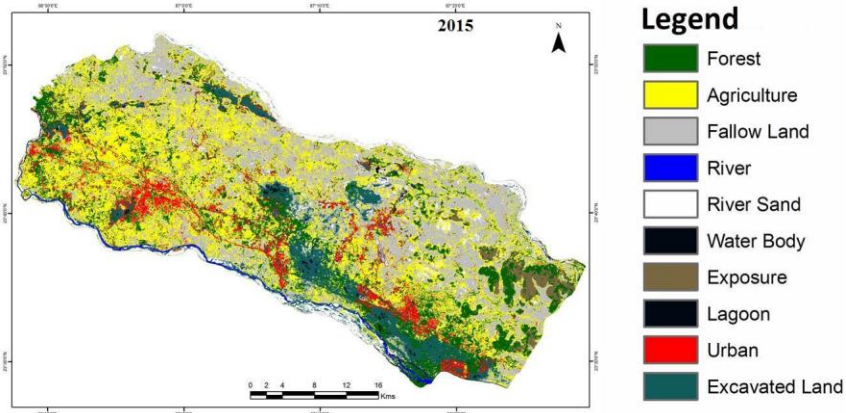


Figure 3.2.3: Landscapes map of 2015, Raniganj coalfield

3

.3 Ground Truth and Training Data Map and Photographs

With the help of Google Earth and GPS device (Garmin 72H) 950 ground truth data has been gathered for full and accurate characterization of ground truth geographic coordinates, land use and land cover attributes, species information of different landscapes using stratified random sampling method (Steven, 1987). 950 in-situ GPS waypoints are plotted in the study region according to its geographical coordinate value shown in figure 3.3.1. Photographs of different landscapes are collected and linked to the classified map according to its geographical coordinate system with the help of Google Earth in an aim to verify the classified land use land cover map with the actual surface features (Sarkar, A., 2017). Forest and excavated quarry land photograph is taken from Purusattampur area

(23°42'10"N and 87°16' 16"E) and Sonepur Bazari area (23°39'40"N and 87°11'0"E) respectively shown in Figure 3.3.2. Photograph of agriculture and urban is taken from Kandra area (23°25'42"N and 86°42'41"E) and near Barakar railway station and bus stand area (23°54'22"N and 87°03'34"E) respectively shown in figure 3.3.3. Fallow and river sand photograph is taken from Mithali area (23°43'00" N and 87°03'00" E) and river bed of Ajay (23°32'25"N and 86°20'15"E) respectively shown in figure 3.3.4. Photograph of exposure land and water body is captured from Sonepur Bazari area (23°38'26"N and 87°12'12"E) and Dalurband area (23°42'36"N and 87°01'52"E) respectively shown in figure 3.3.5. Photograph of river and mining lagoon is captured from Barakar river (23°59'12"N and 87°04'10"E) and Poidih abandoned mine (23°29'30"N and 87°12'25"E) respectively shown in figure 3.3.6.

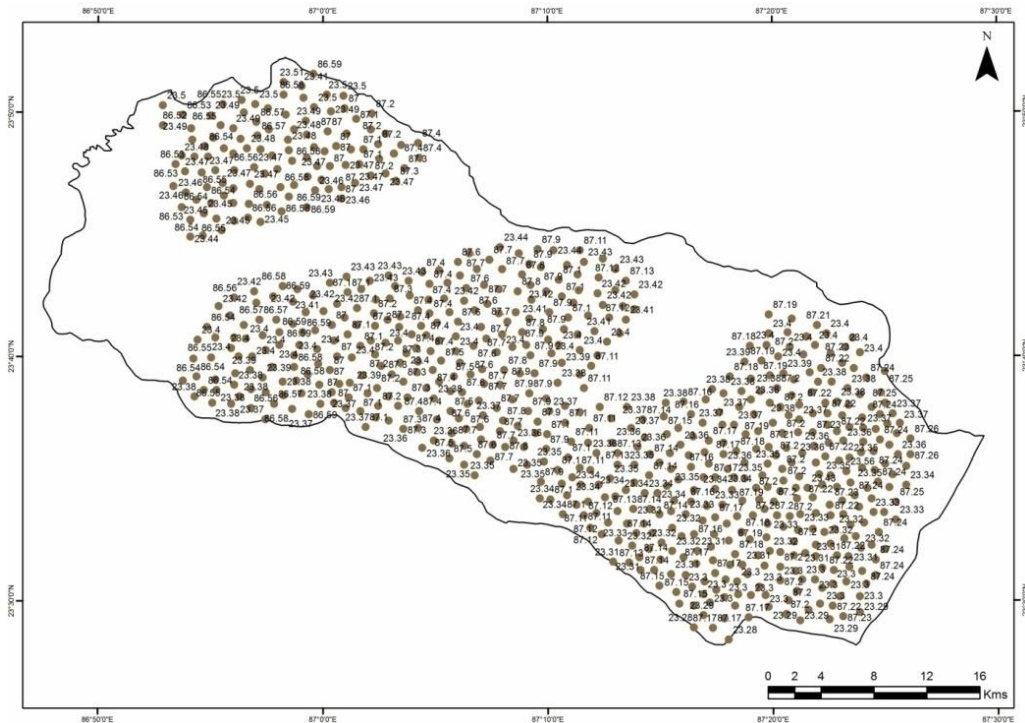


Figure 3.3.1: Ground truth verification waypoints map, Raniganj coalfield



Figure 3.3.2: Landscape photograph of forest and quarry (clock wise), Raniganj coalfield



Figure 3.3.3: Landscape photograph of agriculture and urban (clock wise), Raniganj coalfield



Figure 3.3.4: Landscape photograph of fallow and river sand (clock wise), Raniganj coalfield



Figure 3.3.5: Landscape photograph of exposure and water body (clock wise), Raniganj coalfield



Figure 3.3.6: Landscape photograph of river and mining lagoon (clock wise), Raniganj coalfield

3.4 Accuracy Assessment

This work is done in ERDAS Imagine software followed by classification tab and accuracy assessment tool. The accuracy assessment algorithms are shown in table 3.4.1. Firstly stratified random sampling method is used to furnish the 878 ground truth reference data. These ground truth points are overlain on the land use land cover map and value is extracted (Kuemmerle, et al., 2006). After that a confusion matrix is generated and placed such that

class membership determined by ground truth values are along the x-axis, and class membership determined by image classification is along the y-axis (Green, 1999). When placed this way, correct values fall along the major diagonal of the matrix (Doktoringenieur, G., Buchroithner, M., Dresden, T.U. & Prof, K. 2010). Incorrectly classified values lie in the off diagonal areas of the matrix; such that it is apparent which class they are confused with (Neill, R.V.O., Krummel, J.R., Gardner, R.H., Sugihara, G.,

et al. 1988). Field data for validation is not available for 1973, 1992, 2002 and 2010. So it is assumed that a similar accuracy is achieved using the same methods from the 2015 land use land over map

(Green et al., 1994). Accuracy result for the land use land cover map of 1973, 1992, 2002, 2010 and 2015 is shown in table 3.4.2, 3.4.3, 3.4.4, 3.4.5 and 3.4.6 respectively.

Table 3.4.1: Algorithms for accuracy assessment, Raniganj coalfield

Overall Accuracy	$100 \times \frac{\text{Total number of correctly classified pixels (diagonal)}}{\text{Total number of reference pixel}}$
User Accuracy	$\times 100 \frac{\text{Number of correctly classified pixels in each category}}{\text{Total number of classified pixels in that category (row total)}}$
Producer Accuracy	$\frac{\text{Number of correctly classified pixels in each category}}{\text{Total number of classified pixels in that category (column total)}} \times 100$
Kappa Coefficient (T)	$\frac{\text{Total Sample} \times \text{Total Corrected Sample} - \sum (\text{Column total} \times \text{Row total})}{\text{Total Sample}^2 - \sum (\text{Column total} \times \text{Row total})}$

Table 3.4.2: Confusion matrix for accuracy assessment of LULC map 1973, Raniganj coalfield

Classified Data	LULC Classes	Reference Data								Users accuracy (%)		
		F	AL	FL	R	RS	WB	E	L		U	
	F	1120	65	32		3		21		1241	90.24	
	AL	15	1250	65	4	5	7	6		1356	92.18	
	FL	45		2	2					1057	87.04	
	R	11	21	920			34		37	629	76.31	
	RS	6	12	5	480	9	102	10		606	76.31	
	WB	15	3	42	9	524	16		6	510	86.47	
	E	18	25	25	8	4	425	8		408	93.0	
	L	18	30	3	6		19	285		486	69.85	
	U	5	23					4	6	1593	86.63	
	EL		5					4	421	20	552	91.46
	Total	1235							1467	8408	98.73	
			1434	1092	507	545	603		7	545		
Producer Accuracy (%)		90.69	87.17	84.25	94.67	96.15	70.48	87.42	90.34	97.28		
		98.91										
											Overall Accuracy: 88.46%	
											Kappa Coefficient: 0.81	

Table 3.4.3: Confusion matrix for accuracy assessment of LULC map 1992, Raniganj coalfield

Classified Data	LULC	Reference Data								Users accuracy
		F	AL	FL	R	RS	WB	E	L	

Classes	EL	Total								(%)	
F	1420	32	36			5		23		1516	93.67
AL	21	1020	65	6	8		11	8		1146	89.01
FL	54		2	5						1052	86.12
R	2	31	906				36		25	760	80.26
RS	4	15	5	610	9		98	21		901	91.68
WB	8	4	42	5	826	15			5	530	86.42
E	20	36	5	6		34	389	7	3	481	68.61
L	9	15						8		1438	87.83
U		4						9	498	466	99.09
EL									25	1468	471
Total	1538								1425	8850	98.28
		1178	1081	635	854	652		450	523	1468	471
Producer Accuracy (%)	92.32	86.59	86.9	83.81	96.72	69.60	86.44	95.22	97.07		
Overall Accuracy: 88.14%											
Kappa Coefficient: 0.86											

Table 3.4.4: Confusion matrix for accuracy assessment of LULC map 2002, Raniganj coalfield

LULC Classes	Reference Data										Users accuracy (%)
	F	AL	FL	R	RS	WB	E	L	U		
F	1725	52	29		8		25			1839	93.80
AL	25	1230	50	10	12	4	3			1337	92.00
FL	69		2	1						1059	85.74
R	11	25	908			32		25		789	79.21
RS	4	32	5	625	9	102	5			749	92.12
WB	5	4	25	2	690	21		3		689	87.23
E	21	32	36	5	5	601	5			467	82.44
L	36	20	4	9		36	385		7	548	85.58
U		36	15				6			1398	96.92
EL			7			7	469	36		594	99.16
Total	1896							1355		9469	
		1417	1057	651	724	796		5	589		
Producer Accuracy (%)	90.98	86.80	85.90	96.00	95.30	75.50	90.59	90.37			
Overall Accuracy: 90.04%											
Kappa Coefficient: 0.88											

Table 3.4.5: Confusion matrix for accuracy assessment of LULC map 2010, Raniganj coalfield

LULC Classes	Reference Data										Users accuracy (%)
	F	AL	FL	R	RS	WB	E	L	U		
F	1654	59	36		6		25			1780	92.92
AL	29	1235	68	11	21	3	9			1397	88.40
FL	42		8	13						1257	89.10
R	11	25	1120			24		46		592	71.24
RS	13	16	2	421	15	102	25			973	87.98
WB	2	3	42	12	856	35		12		502	84.66
E	7	14	36	9	6	425	10			382	74.60
L		30	13	8		36	285		1	653	
		29					2			1451	

U	13	12					8	589	20	591	90.20
EL									1426	9578	98.28
Total	1771	1423	1317	461	904	625			9	582	98.48
Producer Accuracy (%)	93.39	86.79	85.04	91.32	94.69	68	352	645	1476	597	96.61
Overall Accuracy: 88.424%											
Kappa Coefficient: 0.84											

Table 3.4.6: Confusion matrix for accuracy assessment of LULC map 2015, Raniganj coalfield

Classified Data	LULC Classes	Reference Data								Users accuracy (%)			
		F	AL	FL	R	RS	WB	E	L		U		
	EL		Total										
	F	1612	48	21		4			17			1702	94.7
	AL	20	1180	57	5	7	8	5				1290	91.5
	FL	56		5	3							1146	88.0
	R	9	19	1008			29			34		695	75.3
	RS	5	20	3	523	9	124	10				740	96.8
	WB	9	2	36	8	716	12			2		544	93.0
	E	13	17	28	2	2	506	4				544	93.0
	L	13	35	7	4		23	315		2		408	77.2
	U	8	25						5			466	90.8
	EL		8					6	423	20		1593	95.5
	Total	1732							1522			702	97.2
			1354	1160	542	734	677		3	682		9286	
Producer Accuracy (%)		93.1	87.1	86.9	96.5	97.5	74.7	88.7	96.8				
Overall Accuracy: 90.74%													
Kappa Coefficient: 0.92													

3.5 Landscape Fragmentation

Entire tasks are done in Arc GIS 10.2 and Fragstats 4.2 software. Individual land use land cover map is converted from raster to polygon in Arc GIS following arc tool box/3d analyst tool/conversion/from raster algorithm. Then fragmentation is computed using class analyzing tool and landscape analyzing tool respectively from patch

analyst tool following spatial statistics/ analyzed by class or landscape. In Fragstats software these work is done using grid method followed by input layer and analysis tab. Patch metrics, class metrics and landscape metrics indices are calculated. Area edge, shape, core area, contrast, aggregation and diversity are also calculated for different indices. The selected landscape metrics are shown in table 3.5.1.

Table 3.5.1: Selected landscape indices for Raniganj coalfield area

Landscape Indices	Algorithm	Description
Number of Patches	$NumP = n_i$	This describes number of patches in each class type and the growth of particular patches in the region (Ng, 2006).
Class Area	$CA = \sum_{j=1}^n a_{ij}$	This is the total class area for individual land use land cover. It also measures land use land cover combination (Suocheng, D., 2013)
Percentage of Land	$PLAND = \frac{CA}{TA}$	This is the measure of the landscape composition (Ruishan, H., 2013). It describes sum of the areas of all patches divided by total landscape area.

Largest Patch Index	$LPI = \frac{\max_{j=1}^n (a_{ij})}{A}$	This is single largest patch at the class level which gives indication of fragmentation, homogeneity, dominance and changes within a landscape (Yu, 2006). 100 describe landscape consists of a single patch while 0 denotes largest patch type is absent.
Patch Density	$PD = \frac{n_i}{A} (10000) (100)$	This is a measure of fragmentation of a patch type or landscape (Mairota, 2013). higher value indicates fragmented growth and vice versa.
Total Edge Length	$TE = \sum_{k=1}^M e_{ik}$	This is an absolute measure of total edge length for particular patch type. Higher value indicates larger continuous patches and vice versa (Lion, 2004).
Edge Density	$ED = \frac{\sum L}{TA} \times 10000$	This is the ratio of total edge distance to the total Area (Poorva, 2006). Zero edge density indicates no class of the landscape.
Mean Patch Size	$MPS = \frac{NP}{TA}$	This is the average size of patches of a land use class and denotes landscape configuration and fragmentation (Millington et al., 2003).
Patch Size Coefficient of Variance	$PSCoV = \frac{PSSD}{MPS}$	This is the coefficient of variation of patches. It measures relative variability about the percentage of the mean not absolute variability (Hu, 1970).
Patch Size Standard Deviation		This is an absolute standard deviation measure of mean patch areas and difference in patch size among patches (NG, 2006).
Mean Shape Index	$MSI = \sum \frac{PA}{A}$	This is a measure of average patch shape for a particular patch type or for all patches in the landscape (Li et al., 2004).
Area Weighted Mean Shape Index	$AWMSI = \frac{MSI}{PA}$	This is mean patch shape complexity, weighted by patch area (Sadhu K., 2012). 1 AWMSI indicates all patches are circular while increasing value indicates patches become complex in shape.
Mean Perimeter Area Ratio	$MPAR = \frac{\sum PA}{AR} \times NumP$	This is the measure of shape complexity It is the function of sum of each patch perimeter, area ratio and number of patches (Mairota, 2013).
The Shannon Diversity Index	$SHDI = - \sum_{i=1}^M (p_i \cdot \ln p_i)$	This is relative measure of patch diversity, heterogeneity and fragmentation at class level of the community (Mairota et al., 2013). Higher index value indicates more diverse landscape.
Shannon Evenness Index	$SHEI = \frac{M}{-\sum_{i=1}^M (p_i \cdot \ln p_i) / \ln m}$	This is a measure of patch distribution or abundance and only available at the landscape level (Li et al., 2004). 0 SEI indicates low patch distribution while 1 denotes more even distribution

13 class level indices and 2 landscape level indices for Raniganj opencast mining area are computed and displayed in table 3.5.2 and 3.5.3 respectively.

Table 3.5.2: Class level indices from 1973 to 2015, Raniganj coalfield

Landscape Indices	Year	Forest	Agricultural Land	Fallow Land	River	River Sand	Water Body	Exposure	Lagoon	Urban	Excavated Land
Class Area	1973	38143.1	55253.65	35256.5	4327.42	4165.68	925.82	3917.34	692.27	3552.24	7264.53
				2							

Number of Patches	199	29708.9	62113.8	32124.9	4018.95	4963.41	768.24	6723.72	884.7	8895.65	10764.5
	2										
	200	27288.6	49115.6	34421.4	1838.07	8491.05	766.53	9862.74	1101.6	11219.5	15067.2
	2										
	201	28193.1	38693.7	41045.9	961.02	8043.3	762.48	9575.28	1297.77	16020	10854
	0										
	201	22096.8	44858.6	45843.2	717.75	8870.67	712.71	5232.68	1678.69	19648.7	13764.6
	5									2	
	197	22216	33061	13080	6408	689	2794	14388	1917	7658	9441
	3										
Percentage of Land	199	41415	32735	19688	5952	821	2319	17994	2450	19178	13804
	2										
	200	44170	31855	22923	1462	3454	2611	24696	3163	21226	17147
	2										
	201	53172	36730	25175	1242	6043	3104	34197	1873	32263	26033
	0										
	201	59981	37166	26290	1056	7868	3090	25239	2108	32603	17147
	5										
	197	25.12	36.31	23.64	3.24	3.63	1.03	3.34	0.23	2.68	5.42
	3										
Patch Density	199	18.47	38.58	19.97	2.50	3.08	0.48	4.18	0.55	5.52	6.68
	2										
	200	17.14	30.86	21.63	1.15	5.33	0.48	6.20	0.69	7.05	9.47
	2										
	201	18.13	24.90	26.41	0.62	5.17	0.49	6.15	0.83	10.31	6.98
	0										
	201	13.52	27.45	28.05	0.44	5.43	0.44	3.20	1.03	12.03	8.42
	5										
	197	38.236	28.256	19.256	6.526	0.652	2.102	13.654	1.201	5.625	12.201
	3										
Largest Patch Index	199	32.564	30.215	17.624	5.216	0.846	1.956	18.256	1.950	16.256	15.265
	2										
	200	40.231	26.364	16.102	1.365	6.126	2.620	28.245	2.695	26.358	19.856
	2										
	201	34.125	27.698	12.365	1.102	4.021	2.056	14.652	1.186	26.254	7.658
	0										
	201	17.259	29.652	20.362	0.980	6.856	2.421	3.654	1.265	16.859	14.521
	5										
	197	18.201	9.526	7.269	1.201	0.039	0.524	2.654	0.216	1.624	2.126
	3										
Total Edge	199	14.256	11.246	6.387	0.952	0.080	0.236	6.912	0.310	4.325	4.987
	2										
	200	20.354	7.246	4.215	0.547	1.210	0.856	8.856	0.895	8.654	7.568
	2										
	201	16.325	7.698	2.321	0.432	0.562	0.123	3.568	0.120	8.452	1.268
	0										
201	6.248	10.564	7.658	0.215	1.625	0.756	1.003	0.256	5.846	2.689	
5											
197	1734175	18226821.	998899	1787515.	583497.	63047	274429	415808.	136248	356654	
3	6.1	49	2.8	88	05	8	8.5	8	4.1	7.8	
199	1350714	20489816.	910173	1660097.	695237.	52316	471031	531391.	341198	528487	
2	8.7	40	2.4	41	13	7	2.4	71	3.9	1.4	
200	1591350	17846220	938502	709140	202992	63000	772182	709260	778008	814200	

	2	0		0		0	0	0	0	0	0
	201	1525269	13695074.	720990	640936.7	137764	53229	466769	417124.	867512	338549
	0	8.3	47	1.9	75	7.8	1	1.9	10	0.1	3.5
	201	7968584.	17937756.	127741	383651.0	253339	58460	132644	401368.	539948	491502
	5	76	08	15	1	3.8	5	4.8	93	0.7	8.1
Edge Density	197	55.335	58.168	31.826	5.696	1.854	2.000	8.756	1.322	4.344	11.382
	3										
	199	43.106	65.391	29.0473	5.298	2.218	1.669	15.032	1.695	10.889	16.866
	2										
	200	50.3586	56.474	29.699	2.244	6.423	1.993	24.435	2.244	24.620	25.765
	2										
	201	48.267	43.338	22.815	2.028	4.3596	1.684	14.771	1.32	27.4526	10.713
	0										
	201	25.115	56.535	40.261	1.209	7.984	1.842	4.180	1.265	17.017	15.491
	5										
Mean Patch Size	197	0.5824	0.5983	0.3709	1.4807	0.1653	3.0178	3.6729	2.7691	2.1558	1.2996
	3										
	199	1.3940	0.5270	0.6128	1.4809	0.1654	3.0185	2.6761	2.7693	2.1558	1.2823
	2										
	200	1.6186	0.6485	0.6659	0.7953	0.4067	3.4062	2.5039	2.8712	1.8918	1.1380
	2										
	201	1.8859	0.9492	0.6133	1.2923	0.7513	4.0709	3.5713	1.4432	2.0139	1.8846
	0										
	201	2.7144	0.8285	0.5734	1.4712	0.8869	4.3355	4.8233	1.2557	1.6592	1.8913
	5										
Mean Shape Index	197	1.296	1.183	1.370	1.356	1.261	1.263	1.252	1.246	1.256	1.272
	3										
	199	1.323	1.332	1.342	1.255	1.415	1.274	1.281	1.270	1.242	1.280
	2										
	200	1.243	1.346	1.317	1.367	1.255	1.221	1.249	1.229	1.243	1.281
	2										
	201	1.317	1.330	1.344	1.376	1.307	1.258	1.297	1.259	1.289	1.299
	0										
	201	1.334	1.362	1.343	1.317	1.291	1.211	1.265	1.21	1.273	1.267
	5										
Area Weighted Mean Shape Index	197	8.293	22.181	10.162	8.226	2.501	2.603	1.666	2.558	0.877	3.792
	3										
	199	6.4555	28.661	9.256	7.641	2.982	2.158	2.856	3.271	2.197	5.619
	2										
	200	6.214	26.609	7.368	7.283	8.480	1.597	2.046	2.708	3.653	5.221
	2										
	201	5.321	19.609	10.573	4.404	6.179	1.646	2.474	2.016	3.095	6.654
	0										
	201	9.052	24.411	13.652	3.454	5.099	1.528	5.874	1.638	4.155	9.030
	5										
Patch Size Coefficient of Variance	197	2363.65	8340.468	3657.92	3033.215	482.584	489.27	836.635	752.756	323.052	1301.80
	3						7			4	
	199	1841.280	9376.264	3333.11	2817.434	575.333	406.53	1436.46	962.866	809.257	1929.67
	2			8			8	0		6	
	200	2122.029	5178.708	1569.06	1456.741	3804.18	213.05	431.978	962.265	1195.01	1309.01
	2			6		4	2			5	0
	201	1427.099	2731.143	2560.32	819.279	2217.86	262.77	868.819	453.559	833.837	2025.09
	0			5		7	4			2	

Patch Size	201	1132.689	3088.358	3190.55	655.091	1959.53	313.48	2880.01	467.412	1228.51	3381.01
	5			2		8	0	9		0	0
Standard Deviation	197	16.690	140.549	50.484	19.381	28.535	1.578	2.114	2.629	0.674	6.748
	3										
Mean Perimeter Area Ratio	199	13.162	158.742	46.440	18.965	34.849	1.313	3.635	3.362	1.690	10.040
	2										
	200	10.361	79.847	23.447	18.314	55.842	0.527	1.245	3.351	4.112	7.576
	2										
	201	11.732	32.472	67.877	13.612	51.568	0.687	4.513	1.649	4.071	21.604
	0										
	201	11.138	42.216	55.831	5.938	20.969	0.762	21.266	1.457	5.535	27.076
	5										
	197	1315.82	1344.857	1437.41	1273.875	1126.56	1320.1	1502.46	1389.40	1402.14	1382.71
	3			0		1	1	1	5	6	6
	199	1274.110	1287.594	1309.73	1183.072	1081.36	1273.5	1432.27	1359.82	1350.15	1308.82
	2			3		3	2	8	6	4	4
	200	1151.218	1073.240	1079.85	1073.070	1116.73	1136.8	1126.80	1146.74	1143.48	1109.61
	2			0		8	3	7	0	6	9
	201	1225.643	1183.373	1199.93	1164.910	1286.98	1257.6	1278.14	1267.19	1231.21	1146.51
	0			3		3	3	5	5	5	7
	201	1207.298	1212.615	1215.39	1198.112	1260.59	1192.4	1330.56	1278.06	1257.13	1258.92
	5			8		7	7	4	0	9	8

Table 3.5.3: Landscape level indices from 1973 to 2015, Raniganj coalfield

Year	Shannon Diversity Index	Shannon Evenness Index
1973	1.453	0.606
1992	1.524	0.635
2002	1.536	0.640
2010	1.610	0.671
2015	1.612	0.672

4. DISCUSSION AND FINDINGS

Detailed statistical information of class area and percentage of land is shown in figure 4.1. Class area clearly indicates that there is a major temporal change in forest followed by agriculture and fallow. There is reduction in forest, agriculture, water body and river in 1973 to 2015. Contrary, area under fallow, river sand, exposure, lagoon, urban and excavated is increased in the abovementioned time period in northern and eastern parts of this coalfield namely Purushottampur, Sonapur and Pandaveswar area. Therefore it can be said that the part of forest cover transformed into agriculture or fallow or excavated land. Result of percentage of land indicates that agricultural land occupies highest percentage of

land followed by fallow and forest. Contrary, water body occupies lowest percentage of land followed by river and lagoon. In 1973, the forest class covered an area of 25.23%, but in 2015 it decreased to 13.52%. The area covered by agricultural land also decreased from 36.14% in 1973 to 27.44% in 2015. The river is decrease from 3.02% in 1973 to 0.43% in 2015. Fallow land is increased by 10.23% in past 50 years. This shows that the area under the forest is turn in to the fallow, agriculture and urban land. Urban shows the increase by 2.32% in 1973 to 12.02% in 2015. West and North of this coalfield Satgram, Kajora and Sripur exhibits maximum agriculture and fallow land.

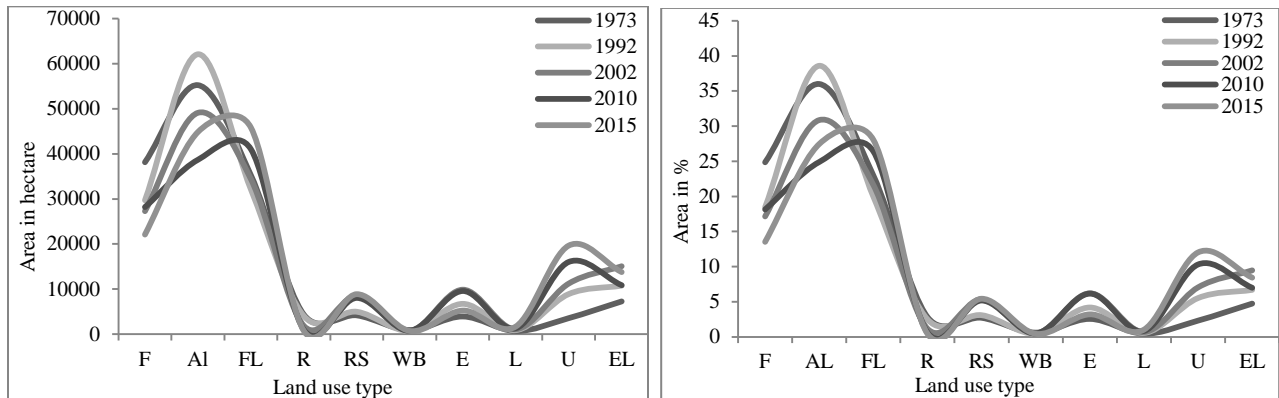


Figure 4.1: CA and PLAND 1973 to 2015 (clock wise), Raniganj Coalfield

Detailed statistical information of number of patch and patch density is shown in figure 4.2. Numbers of forest patches have increased from 22216 in 1973 to 59981 in 2015. Many forest patches isolated and converted into agriculture, fallow, quarry or urban in recent times near north-western area i.e. Sodepur, Slanpur and Pandaveswar. Number of patches for agriculture is increased from 33061 to 36730 during 1973 to 2015 is due to conversion of farmland into grassland. Number of fallow patches increased 25175 to 26290, river sand patches increased 689 to 7868 and urban patches increased 7658 to 212226 in 1973 to 2015 respectively near Asansol and Raniganj. Agriculture patches have increased slightly because of aggregation of smaller fields into larger ones. Urban and excavated patches have increased due to

growing urbanization and mining activities (Batistella, M., Robeson, S. & Moran, E.F. 2003). Only river patches are decreased from 6408 to 1056 in 1973 to 2015 near river Ajay and Damodar. Acute increase in the number of patches indicates fragmentation. Patch density for forest, agriculture, river, exposure is significantly decreased with time. The major decreased is observed in forest 38.236 to 17.259 and river 6.526 to 0.980 since 1973 to 2015. There is a little increase in patch density for agriculture 28.256 to 29.652 and fallow 19.256 to 20.262. Patch density drastically accelerated for river sand 0.652 to 6.856, urban 5.626 to 16.859 and excavated land 12.201 to 14.521. Higher patch density indicates low fragmentation within these land uses.

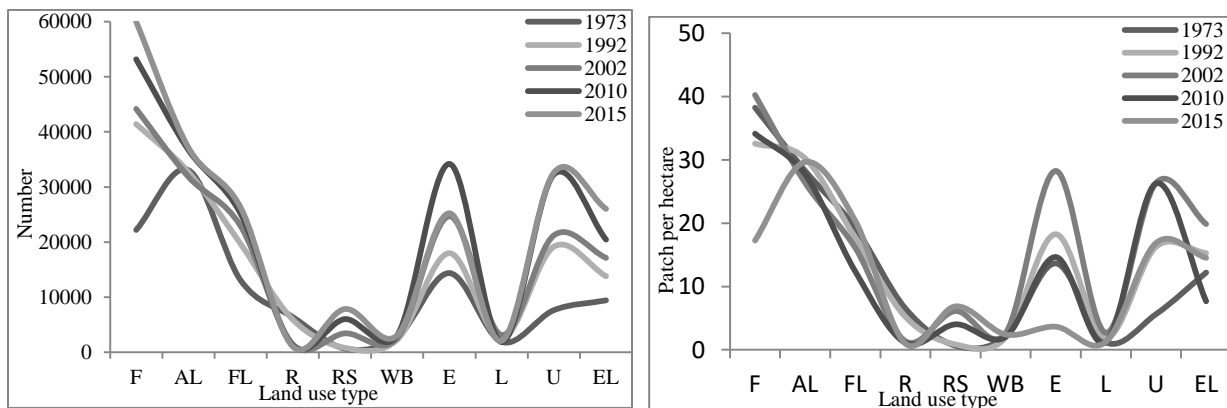


Figure 4.2: NP and PD 1973 to 2015 (clock wise), Raniganj Coalfield

Figure 4.3 shows temporal changes and detailed statistical information in total edge and edge density. There is a significant increase in total edge for fallow land, river sand, urban and excavated. Fallow

increased 9988999.8 hectare to 127774115.2 hectare where urban increased 1362484.1 hectare to 5399480.7 hectare during 1973 to 2015 near Kunstoria, Sripur, Satgram and Sodepur area.

Agriculture, exposure and lagoon do not exhibit much difference in total edge. During the period forest, river and exposure edges have decreased drastically. Forest decreased 17341756.1 hectare to 7968584 hectare, river 1787515.8 hectare to 383651.1 hectare and exposure decreased 2744298.5 hectare to 13264448.6 hectare in 1973 to 2015 respectively.

There is an acute decrease of edge density for forest, agriculture, river, water body and exposure. Forest declined from 55.33 meter/hectare to 25.11 meter/hectare, river decreased from 5.69 meter/hectare to 1.20 meter/hectare and exposure

declined from 8.75 meter/hectare to 4.18 meter/hectare during 1973 to 2015 respectively. This result denotes fragmentation in these land uses due to opencast mining and human pressure on existing land. Some land use exhibits sharp increase in edge density. Like fallow 31.82 meter/hectare to 40.26 meter/hectare, river sand 1.85 meter/hectare to 7.98 meter/hectare, urban 4.34 meter/hectare to 17.01 meter/hectare during 1973 to 2015 respectively. It is happened due to rapid urbanization process and industrial development in Raniganj coalfield area near Kulti, Asansol, Raniganj, Barakar and Disergarh.

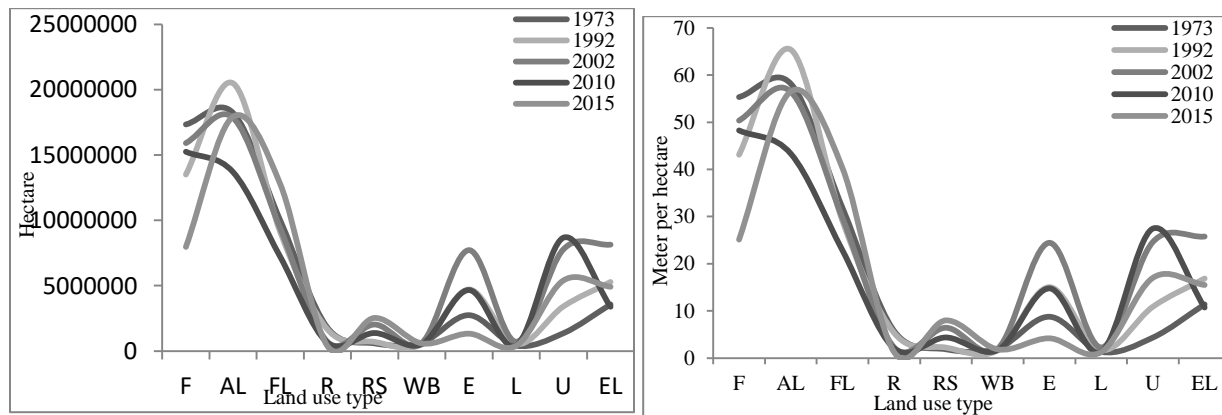


Figure 4.3: TE and ED 1973 to 2015 (clock wise), Raniganj Coalfield

Class level largest patch index and mean patch size is shown in figure 4.4. Forest is the largest patch in each class as a percentage of the total landscape. In 1973, largest patch index for forest was 18.201% of total area and then it decreased to 6.248% of total area in 2015. In 1973, the patches of forest were large and continuous. However, in 2015, the patches are scattered compared to 1992, 2002 and 2010. It is the sign of more prominent fragmentation. Urban largest patch index was 1.624% of total area in 1973 and it increased to 5.846% of total area in 2015. It suggests that urban is increasingly becoming a dominant land use within the landscape. Urban expansion is mainly at the southern part of the study area bordering to Asansol, Durgapur, Barakar, Kulti, Raniganj city area. Largest patch index for agriculture and river sand is increased by about 1%. Largest path index for fallow land is decreased from 7.269% in 1973 to 2.321% in 2010. But it increased to 7.658% in 2015.

In 2010 largest patch index of all land uses are decreased. Henceforth in 2015 the largest patch index for agriculture, river sand, water body, mining lagoon and excavated slightly increased and landscape becomes more complex with comparison of simple shape in 1973. Decrease in the largest patch size and increase in patches above mentioned land use land cover classes clearly indicate that patches getting clumped and tries to form a single patch therefore landscape is becoming fragmented with an acute rate. Areas covered with vegetation observed a decrease in mean patch size from 2.71 hectare to 0.51 hectare in 1973 to 2015. Contrary urban area witnessed an acute increment from 1.65 hectare to 2.45 hectare in 1973 to 2015. Forest, agriculture, river, water body, lagoon are undergoing drastically conversion and fragmentation into quarry, fallow and urban near Jhanjra, Bankola, Kenda and Sonepur Bazari. Subsequent decrease in mean patch size in major land

use classes which are associated with increased fragmentation (Li et al. 2004). It has been concluded that mean patch size is likely the most crucial

indicator of fragmentation (McGarigal and Marks, 1995), therefore I suggest Fragmentation has increased in Raniganj coalfield area since 1973.

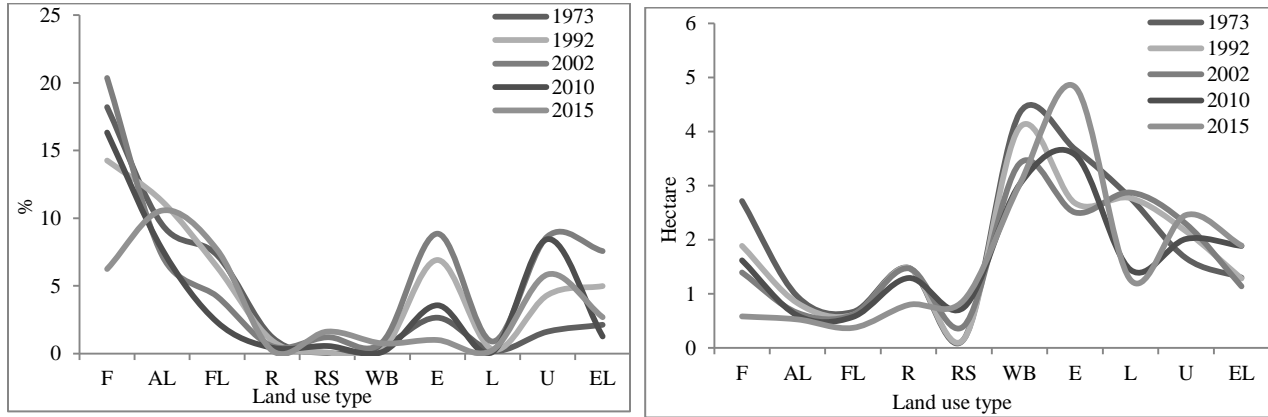


Figure 4.4: LPI and MPS 1973 to 2015 (clock wise), Raniganj Coalfield

Detailed about mean shape index and area weighted mean shape index is shown in figure 4.5. Result suggests that there is little change in mean shape index for all land uses. Forest increased from 1.29 to 1.33, agriculture 1.18 to 1.36, river sand 1.26 to 1.29, urban 1.25 to 1.27 in 1973 to 2015 which indicates patch shape irregularity and fragmentation. Fallow, river and mining lagoon exhibits a decrease of 1.37 to 1.34, 1.35 to 1.31 and 1.24 to 1.21 in 1973 to 2015 respectively which are less fragmented and less irregular. The area weighted mean shape index shows small change for forest from 8.29 in 1973 to 9.05 in 2015 which suggest increasing trend in shape complexity and fragmentation. The area weighted

mean shape index for agriculture, fallow, river sand, excavated land and urban has increased in north and western area. Such changes indicate an expansion of these land uses around urban and coalfield areas of Raniganj coalfield. Agriculture increased from 22.18 to 24.41 and urban from 0.87 to 4.15 in 1973 to 2015 respectively. It expresses that inter patch connectivity among these land uses have decreased. This also indicates increase in shape complexity. AWMSI for mining lagoon, water body and river have declined from 2.55 to 1.63, 2.60 to 1.52 and 8.22 to 3.45 in 1973 to 2015 respectively. It indicates that these landscapes tend to be circular in shape and decrease in shape complexity.

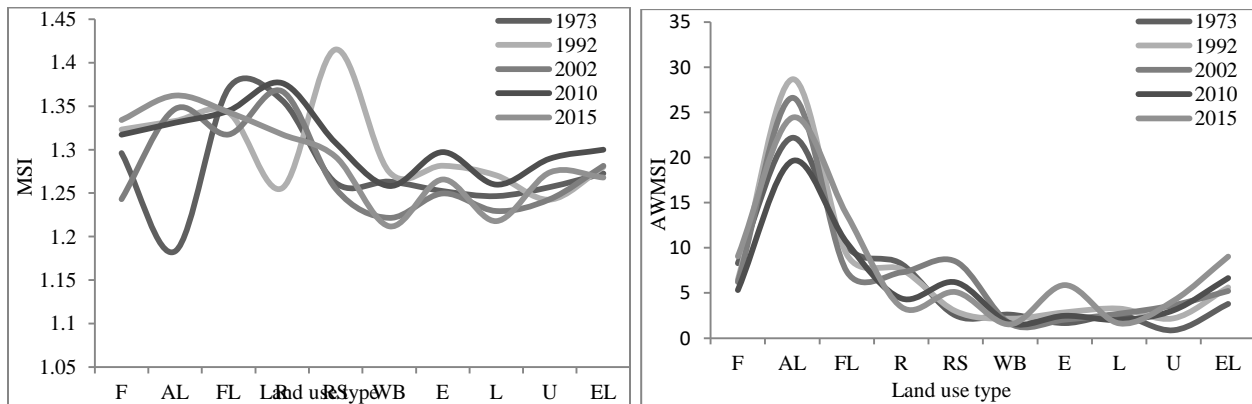


Figure 4.5: MSI and AWMSI 1973 to 2015, Raniganj coalfield

Figure 4.6 shows patch size standard deviation and patch size coefficient of variation. These can be misleading with regards to landscape structure in the absence of information on the number of patches or patch density (Baldi, G. & Puelo, J.M. 2008). Patch size standard deviation for forest, river, river sand, water body and mining lagoon decreased in tiny rate. While fallow exhibits huge decreased in PSSD from 140.54% in 1973 to 42.21% in 2015. This indicates fragmentation growth in these landscapes. There is a huge increase of PSSD for urban and excavated land from 0.67% to 5.53% and 2.11% to 21.26% respectively in the above mentioned study period.

This means urban and excavated landscapes becoming dominant in Raniganj coalfield area. Patch size coefficient of variation is computed due to some drawback of patch size standard deviation. Patch size coefficient of variation is acutely declined for forest 2363.65 hectare to 1132.68 hectare, agriculture 8340.46 hectare to 3088.35 hectare, and river 3033.21 hectare to 655.09 hectare. Water body and mining lagoon decreased in a small rate. There is a sharp increase of PSCoV for excavated land, urban and river sand. Urban area dominantly increased from 323.05 to 1228.25 during the period.

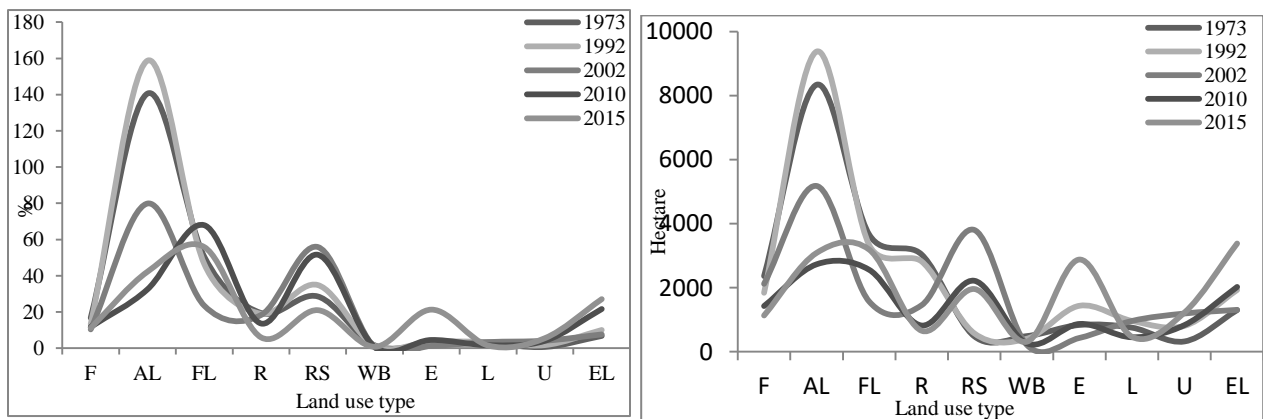


Figure 4.6: PSSD and PSCoV 1973 to 2015 (clock wise), Raniganj coalfield

Mean perimeter area ratio is shown in figure 4.7. Except of river sand, MPAR is declined for all land use categories. It indicates whole landscape has become more complicated and fragmented. Fallow exhibits acute decreased from 1437.41 hectare in 1973 to 1215.39 hectare in 2015. There is an increase of mean perimeter area ratio for river sand from 1126.56 hectare in 1973 to 1260.59 hectare in 2017. It can be said that river sand will be increased in Raniganj coalfield area in terms of mean perimeter area ratio.

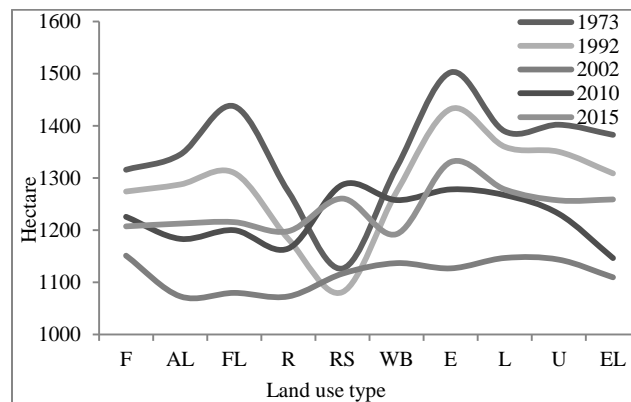


Figure 4.7: MPAR 1973 to 2015, Raniganj coalfield

Shannon diversity index and Shannon evenness index is only computed landscape level in order to measure the fragmentation process as a whole shown in figure 4.8. Indeed SDI and SEI is likely skewed due to many small patches like water body, excavated land, exposure and mining lagoon in Raniganj coalfield area (Areendran, G., Rao, P., Raj, K., Mazumdar, S., et al. 2013). The increase in the Shannon diversity index from 1.45 in 1973 to 1.61 in 2015 indicates that landscape heterogeneity and diversity increased in Raniganj coalfield. It also means proportional

distribution of different patch in the landscape therefore landscape becomes evenly distributed and fragmented. Shannon evenness index increased from 0.60 in 1973 to 0.67 in 2015. The increase in the SEI indicates that the distribution of landscape patches is more even in 2015 than it was in 1973. Outcome of these two indices clearly suggest pattern of spatial change in successive years. If these trends will carry on therefore landscape of Raniganj and adjoining become more heterogeneous and scattered.

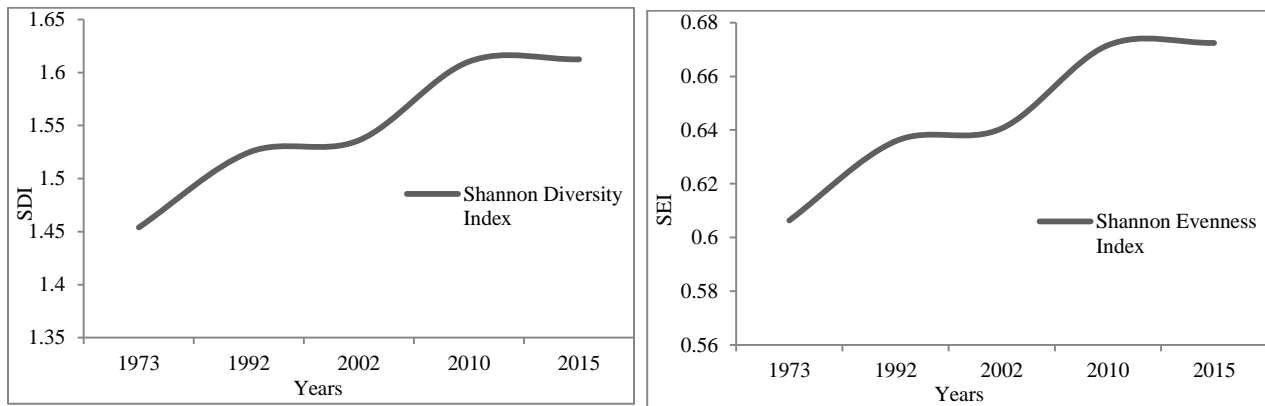


Figure 4.8: SDI and SEI 1973 to 2015 (clock wise), Raniganj coalfield

5. CONCLUSION

In recent time opencast mining and associated development activities are recognized as the most significant factor in order to widespread fragmentation of the landscape in Raniganj coalfield area. After assessing above mentioned results it is clear that forest patches have converted into numerous small patches and isolated in recent times. Contrary urban, fallow and excavated land will be dominated because of their increasing patch size. This huge level of land use fragmentation in Raniganj coalfield area is occurred due to extension of mining areas, development of infrastructure and residential complexes of mining industry and thermal power plants (Ampofo, S., Sackey, I. & Ampadu, B. 2016). This intensive analysis indicates that forest, water body and river are acutely fragmented land use. These land uses are more affected in past 40 years because of declining class area, percentage of land, patch density and largest patch size. Forest and river are most prone to future fragmentation. Contrary fallow, agriculture, river sand is moderately fragmented land use because of moderate patch

density, largest patch index and percentage of land. Urban is acutely effective land use in Raniganj coalfield area because of inclining class area, patch density and percentage of land in past 40 years. In the conclusion it can be said that agriculture and urban will dominate this area in near future. Large scale opencast mining, agricultural expansion, land abandonment, illegal small scale mining, deforestation and rapid urbanization predominately occurred in and around the periphery of Raniganj mining area will make the landscape or ecosystem more complex and fragmented in near future (Dupin, L., Nkono, C., Burlet, C., Muhashi, F., et al. 2013).

REFERENCES

- [1] Ampofo, S., Sackey, I. & Ampadu, B. (2016) Landscape Changes and Fragmentation Analysis in a Guinea Savannah Ecosystem : Case study of Talensi and Nabdram Districts of the Upper East region , Ghana. [Online] 8 (1), 41–54. Available from: doi:10.5539/jgg.v8n1p41.
- [2] Areendran, G., Rao, P., Raj, K., Mazumdar, S., et al. (2013) Land use / land cover change dynamics

- analysis in mining areas of Singrauli district in Madhya Pradesh, India. 54 (2), 239–250.
- [3] Baldi, G. & Paruelo, J.M. (2008) Land-Use and Land Cover Dynamics in South American Temperate Grasslands. 13 (2).
- [4] Batistella, M., Robeson, S. & Moran, E.F. (2003) Settlement Design, Forest Fragmentation, and Landscape Change in Rondônia, Amazônia. 69 (7), 805–812.
- [5] Brown, D.G., Duh, J. & Drzyzga, S.A. (2000) Estimating Error in an Analysis of Forest Fragmentation Change Using North American Landscape Characterization (NALC) Data. 117 (June 1999), 106–117.
- [6] Csorba, P. & Szabó, S. (2010) The Application of Landscape Indices in Landscape Ecology.
- [7] Das, G. & Das, R. (2016) 'Land Use / Land Cover Status relating the Coal fire of Jharia Coal Field' - An Analytical Case Study by RS-GIS Techniques. 5 (9), 1–11.
- [8] Doktoringenieur, G., Buchroithner, M., Dresden, T.U. & Prof. K. (2010) Assessing processes of long-term land cover change and modelling their effects on tropical forest biodiversity patterns – a remote sensing and GIS-based approach for three landscapes in East Africa.
- [9] Dupin, L., Nkono, C., Burlet, C., Muhashi, F., et al. (2013) Land Cover Fragmentation Using Multi-Temporal Remote Sensing on Major Mine Sites in Southern Katanga (Democratic Republic of Congo). 2013 (June), 127–139.
- [10] Haddad, N.M., Brudvig, L.A., Clobert, J., Davies, K.F., et al. (2015) Habitat fragmentation and its lasting impact on Earth's ecosystems. (March), 1–9.
- [11] G., Raman, R. & Punia, M. (2006) Land Use Dynamics and Landscape Fragmentation in Higher Himalaya.
- [12] Hochschild, V., Shen, J., Wang, H., Koch, J., et al. (n.d.) ENVIRONMENTAL LAND USE PLANNING Edited by Seth Appiah-Opoku.
- [13] Huang, J., Tu, Z. & Lin, J. (2017) Land-use dynamics and landscape pattern change in a coastal gulf region, southeast China. [Online] 4509 (February). Available from: doi:10.1080/13504500902771891.
- [14] Jaybhaye, R.G., Kale, P.K. & Joshi, P. (2016) The Relevance of Geospatial Techniques in the Assessment of Forest Fragmentation of Anjaneri Hill, Nasik District. [Online] 10 (4), 1–10. Available from: doi:10.9790/2402-1004010110.
- [15] Kindu, M., Schneider, T., Teketay, D. & Knoke, T. (2013) Land Use / Land Cover Change Analysis Using Object-Based Classification Approach in Munessa-Shashemene Landscape of. [Online] 2411–2435. Available from: doi:10.3390/rs5052411.
- [16] Kumar, R., Nandy, S., Agarwal, R. & Kushwaha, S.P.S. (2014) Forest cover dynamics analysis and prediction modeling using logistic regression model. Ecological Indicators. [Online] 45, 444–455. Available from: doi:10.1016/j.ecolind.2014.05.003.
- [17] Maitima, J.M., Mugatha, S.M., Reid, R.S., Gachimbi, L.N., et al. (2009) The linkages between land use change, land degradation and biodiversity across East Africa. 3 (10), 310–325.
- [18] Neill, R.V.O., Krummel, J.R., Gardner, R.H., Sugihara, G., et al. (1988) Indices of landscape pattern. 1 (3), 153–162.
- [19] Pradesh, H., Ramachandra, T. V, Kumar, U. & Joshi, N. V (2005) Landscape Dynamics in Western Himalaya - Mandhala.
- [20] R.H.U. & Suocheng, D. (2013) Land Use Dynamics and Landscape Patterns in Shanghai, Jiangsu and Zhejiang. [Online] 4 (2), 141–148. Available from: doi:10.5814/j.issn.1674-764x.2013.02.006.
- [21] Samanta, P., Technical, S., Manager, P. & Consultants, T. (2015) Impact Assessment and Changes Analysis of Land Use / Land Cover Due to Open Cast Coal Mining Activity: A Case Study of Raniganj Coal Field Area. 4 (5), 17–27.
- [22] Sapena, M. & Ruiz, L.A. (2015) Analysis Of Urban Development By Means Of Multi-Temporal Fragmentation Metrics From Lulc Data. [Online] XL (May), 11–15. Available from: doi:10.5194/isprsarchives-XL-7-W3-1411-2015.
- [23] Srivastav, S., Roy, S.K. & Krishnamurthy, P.S. (2016) An Analysis Of Land Use And Land Cover Dynamics And Causative Drivers In A Thickly Populated Yamuna River Basin Of India. 14 (3), 773–792.
- [24] State, J., Kumar, A. & Pandey, A.C. (2013) Evaluating Impact of Coal Mining Activity on Landuse / Landcover Using Temporal Satellite Images in South Karanpura Coalfields and. 2 (1), 183–197.
- [25] Sarkar, A., (2017) Remote Sensing Approach To Define Landscape Dynamics In Raniganj Coalfield Area Through
- [26] Trend Line Analysis, Vol. 08, Issue, 09, pp.5546-5555, September, 2017.